Synthesis, spectroscopic (FT-IR and NMR), Mulliken, MEP, NLO, and HOMO, LUMO analyses of 2-(1H-imidazol-4-yl)-3-(substituted pyridinyl)thiazolidin-4-one

R. Rameshkumar and N. Santhi*

Department of Chemistry, Government Arts College, Chidambaram - 608201, Tamil Nadu, India
*E-mail address: nsaanthi@gmail.com

Abstract

The title compounds, thiazolidin-4-one (**6-10**) were synthesized and characterized by elemental, FT-IR, NMR spectral analyses. The geometry optimization of the title compounds have been carried out using DFT level with B3LYP method using 6-31G(d,p) basis set and are in agreement with the reported values. In addition, Mulliken charge analysis has also been computed at the same level of theory. The analysis of MEP map shows the negative and the positive potential sites. The HOMO and LUMO analyses were used to elucidate information regarding charge transfer within the molecule. The predicted NLO properties show that the title compounds are a good candidate as nonlinear optical material.

Keywords: thiazolidin-4-one, DFT, NLO, HOMO and LUMO.

1. Introduction

Materials with nonlinear optical (NLO) activity discover their utilization as electro-optic switching elements for telecommunication and optical data handling. In the materials including inorganic, organometallic, organic and polymeric, Organic materials were accepting the greatest consideration in solid state inquire about due to their potential significance for nonlinear optical (NLO) [1,2], electro-optic [3], conductor [4], and different applications [5]. Organic compounds are regularly framed by weak vander Waal's and hydrogen bonds and have high degree of delocalization.

Especially in organic nonlinear optical materials the π conjugated frameworks connecting a donor and an acceptor group give the ground state charge asymmetry of the atom which is in charge of the second order nonlinearity. Thiazolidinone is an important scaffold known to be associated with several biological activities. Thiazolidine-4-dione is widely used for designing novel anti-diabetic drugs. This scaffold exhibits a number of activities such as antidiarrheal [6], anticonvulsant [7], antimicrobial [8-10], antidiabetic [11], antihistaminic [12], anticancer [13,14], anti-HIV [15], cyclooxygenase inhibitory [16]. Among all of these, anti-diabetic activity has been widely carried out and a significant number of drugs are already available in the market such as rosiglitazone, pioglitazone, lobeglitazone and troglitazone etc. In addition, thiazolidinones are also known to exhibit a push-pull effects [17,18] and photovoltaic applications [19]. In addition, intramolecular charge transfer in aromatic push-pull molecules has been a subject of interest in several experimental and theoretical studies [20-22]. Recently, some researcher [23-25] studied the energy gap, reactivity sites and hyperpolarisability of thiazolidinones.

Literature survey reveals that, no DFT frequency calculations of 2-(1H-imidazol-4-yl)-3-(substituted pyridinyl) thiazolidin-4-one (**6-10**) have been reported so far. Therefore, consideration of these factors motivated us to study the detailed theoretical and experimental investigation of compounds **6-10**. Density functional theory calculations are also reported to provide excellent details like reactivity behavior, energy gap and NLO effect [26,27]. In present paper, five 2-(1H-imidazol-4-yl)-3-(substituted pyridinyl) thiazolidin-4-one (**6-10**) have been reported to investigate their synthesis, spectral, Molecular structural properties.

In addition, Mulliken, molecular electrostatic potential, frontier molecular orbital energies, and non-linear optical properties have been investigated on title compounds. These calculations are valuable for providing insight into molecular properties.

2. Experimental

2.1. Materials and methods

All chemicals were purchased commercially and used without prior purification. Melting points were determined in open capillary tube and were uncorrected. Elemental analyses were carried out on Variomicro V2.2.0 CHN analyser. FT-IR spectrum of title compounds were recorded on a Shimadzu FTIR spectrophotometer in the range 400-4000 cm^{-1} using the KBr pellets. The ^{1}H NMR spectra were recorded on a BRUKER AVANCE III 400 MHz NMR spectrometer using $CDC1_3$as solvent. Chemical shifts were reported in ppm. Tetramethylsilane (TMS) was used as internal reference for all NMR spectra, with chemical shifts reported in δ units (parts per million) relative to the standard.

2.1.1. General procedure for the synthesis of thiazolidin-4-one (6-10)

The initial 1H-imidazole-4-carbaldehyde and respective primary amine was dissolved in ethanol (100 mL) and a catalytic amount of $InTiO_2$ was added to round bottom flak. Then the mixture was heated to 100 °C for 12h. The $InTiO_2$ was filtered off and the reaction was concentrated *in vacuo* to give compounds **1-5**. The crude imine **1-5** was resuspended in DMF (25 ml) and thioglycolic acid was added and the reaction was heated. The progress of the reaction was monitored by TLC. After the completion of the reaction, the resulting thiazolidin-4-one (**6-10**) was poured on ice, filtered and purified by column chromatography.

2-(1H-imidazol-4-yl)-3-(5-methylpyridin-2-yl)thiazolidin-4-one (**6**)

Grey powder, M.F.: $C_{12}H_{12}N_4OS$; M.P. 154-156°C, 84% yield; Elemental Analysis (%): Calculated: C, 55.37; H, 4.65; N, 21.52; S, 12.32; Experimental: C, 55.25; H, 4.71; N, 21.48; S, 12.22; IR (KBr, cm^{-1}): 3419(υN-H), 3060 (υAr-CH), 2938 (υali.-CH), 1695(υC=O), 1587(υC=N), 1510-1386 (υC=C), 1286 (ν_{C-N}),1238-1139 (βC-H), 1095-553(ΓC-H); ^{1}H NMR (400 MHz, $CDCl_3$, δ ppm): 13.11 (1H, N-H), 7.85-8.34 (5H, Ar), 5.73 (1H, CH, Thiaz.), 2.98 (2H, CH_2, Thiaz.), 2.31 (3H, CH_3).

3-(4-chloropyridin-2-yl)-2-(1H-imidazol-4-yl)thiazolidin-4-one (**7**)

Orange powder, M.F.: $C_{11}H_9ClN_4OS$; M.P. 162-164°C, 86% yield; Elemental Analysis (%): Calculated: C, 47.06; H, 3.23; N, 19.96; S, 11.42; Experimental: C, 47.01; H, 3.41; N, 19.74; S,11.38; IR (KBr, cm^{-1}): 3479(υN-H), 3061(υAr-CH), 2949 (υali.-CH), 1629(υC=O), 1593(υC=N), 1465-1307 (υC=C), 1251 (ν_{C-N}),1192,1111 (βC-H), 1051-748(ΓC-H); ^{1}H NMR (400 MHz, $CDCl_3$, δ ppm): 13.47 (1H, N-H), 7.26-8.02 (5H, Ar), 5.58 (1H, CH, Thiaz.), 3.03 (2H, CH_2, Thiaz.).

3-(2-chloropyridin-3-yl)-2-(1H-imidazol-4-yl)thiazolidin-4-one (**8**)

Orange powder, M.F.: $C_{11}H_9ClN_4OS$; M.P. 170-172°C, 87% yield; Elemental Analysis (%): Calculated: C, 47.06; H, 3.23; N, 19.96; S, 11.42 ; Experimental: C, 46.98; H, 3.42; N, 19.84; S, 11.40; IR (KBr, cm^{-1}): 3479(υN-H), 3061(υAr-CH), 2945 (υali.-CH), 1631(υC=O), 1591(υC=N), 1467-1303 (υC=C), 1247 (ν_{C-N}),1194,1112 (βC-H), 1001-628(ΓC-H); ^{1}H NMR (400 MHz, $CDCl_3$, δ ppm): 13.39(1H, N-H), 7.48-8.04 (5H, Ar), 3.90 (2H, CH_2, Thiaz.).

2-(1H-imidazol-4-yl)-3-(4-methylpyridin-3-yl)thiazolidin-4-one (**9**)

Pale yellow, M.F.: $C_{12}H_{12}N_4OS$; M.P. 144-146°C, 80% yield ; Elemental Analysis (%): Calculated: C, 55.37; H, 4.65; N, 21.52; S, 12.32; Experimental: C, 55.30; H, 4.55; N, 21.46; S,

12.28 ; IR (KBr, cm^{-1}): 3476(υN-H), 3059(υAr-CH), 2947 (υali.-CH), 1649(υC=O), 1514(υC=N), 1462-1303 (υC=C), 1249 (ν_{C-N}),1197,1112 (βC-H), 1070-626(ΓC-H); ^{1}H NMR (400 MHz, $CDCl_3$, δ ppm): 13.31(1H, N-H), 7.45-7.96 (5H, Ar), 5.57 (1H, CH, Thiaz.), 3.03 (2H, CH_2, Thiaz.), 1.63 (3H, CH_3).

3-(5-chloropyridin-2-yl)-2-(1H-imidazol-4-yl)thiazolidin-4-one (**10**)

Orange powder, M.F.: $C_{11}H_9ClN_4OS$; M.P. 168-170°C, 85% yield; Elemental Analysis (%): Calculated: C, 47.06; H, 3.23; N, 19.96; S, 11.42 ; Experimental: 47.02; H, 3.31; N, 19.87; S, 11.40 ; IR (KBr, cm^{-1}): 3479(υN-H), 3059(υAr-CH), 2945 (υali.-CH), 1627(υC=O), 1587(υC=N), 1462-1340 (υC=C), 1246 (ν_{C-N}),1197,1114 (βC-H), 1066-748(ΓC-H); ^{1}H NMR (400 MHz, $CDCl_3$, δ ppm): 13.14 (1H, N-H), 7.60-8.58 (5H, Ar), 3.11 (2H, CH_2, Thiaz.).

2.2. Computational studies

GAUSSIAN 03W [28] software package was used for DFT calculations. Structure optimizations of **6-10** were performed at the Density Functional Theory (DFT) level employing B3LYP/6-31G(d,p) functional theory. In order examine the reactive sites of the synthesized compounds; the Mulliken and molecular electrostatic potential were evaluated. Also, the HOMO-LUMO on optimized structures is accomplished at B3LYP/6-31G(d,p) level computation. Moreover, in order to show nonlinear optical (NLO) activity of studied molecules, the dipole moment, linear polarizability and first order hyperpolarizability were obtained from molecular polarizabilities based on same level theoretical calculations.

3. Results and discussion

3.1. Molecular geometry

The optimized structural parameters such as bond lengths, bond and dihedral angles have been calculated using DFT-B3LYP/6-31G(d,p) level theory. The optimized structure of compounds **6-10** are shown in **Fig.1**. From the results, we can concluded that the C-S bond length of thiazole ring is in agreement with a C(sp^2)-S single bond length. The predicted C=O bond length is good agreement with the standard double bond value of 1.20 Å. The bond angles values indicate that the π electrons in the title molecule are delocalized. These results indicate that the values calculated by B3LYP method are quite consistent with the experimental values. These results indicate that the values calculated by B3LYP method are quite consistent with the experimental values. It is evident from dihedral angle (N8-C2-C9-N15 and N26-C18-N15-C9), the thiazole ring is slightly deviate from the planarity. From these dihedral angles we conclude that imidazole and pyridine are present in same plane. It is important that the greater part of the optimized parameters have marginally larger values than the corresponding experimental ones. The little contrasts can be on the grounds that theoretical calculations suggest isolated particle in gaseous phase while experimental outcomes refer to the molecule in the solid state.

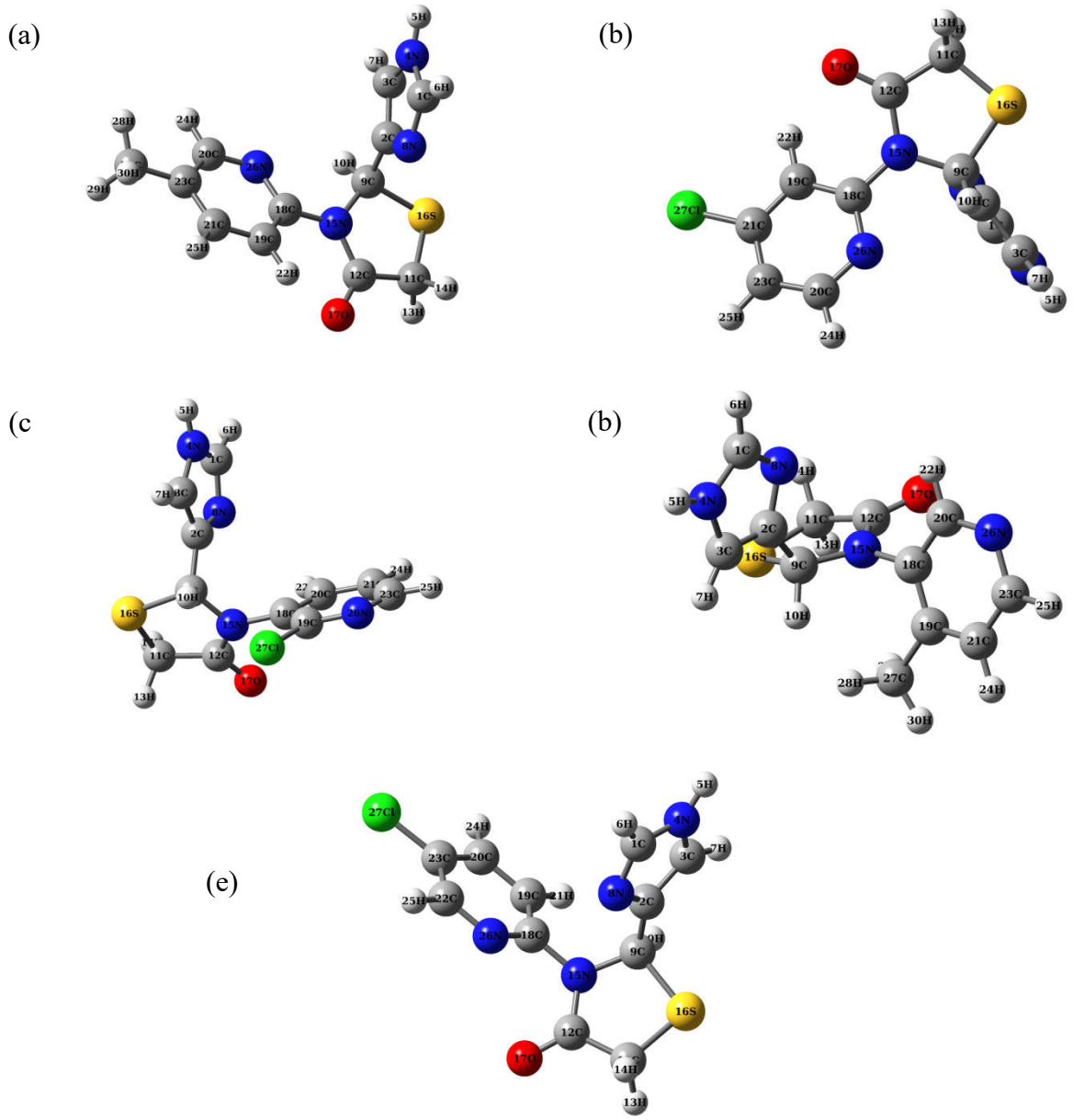

Figs. 1(a-e) The optimized structure of compounds **6-10**

3.2. Mulliken analysis

The Mulliken atomic charges count has an imperative job in the utilization of quantum mechanical computations [29]. As a result of atomic charges, impact dipole moment, polarizability, electronic structure and more a great deal of properties of molecular frameworks. The charge dissemination over the atoms proposes the arrangement of donor and acceptor pairs

including the charge move in the particle. The Mulliken population analysis in **6-10** molecules were calculated using B3LYP/6-31G(d,p) basis set and was listed in **Table 1**. Results from Mulliken charge analysis tables show that atom C1, C2, C3, C12, C18 and S16 has higher positive value in compounds **6-10**. The positive regions are related to nucleophilic reactivity. The negative regions are located around the nitrogen (N4, N8, N15, N26) and oxygen (O17) atoms which are related to electrophilic reactivity. These data clearly show that **6-10** are the most reactive towards substitution reactions.

Table 1 Mulliken atomic charges of **6-10**.

Atom	6	Atom	7	Atom	8	Atom	9	Atom	10
C1	0.41564	C1	0.419905	C1	0.425391	C1	0.425436	C1	0.5919
C2	0.210283	C2	0.207237	C2	0.197881	C2	0.216862	C2	0.160631
C3	0.297536	C3	0.30009	C3	0.301513	C3	0.286802	C3	0.378137
N4	-0.34152	N4	-0.33947	N4	-0.33409	N4	-0.33665	N4	-0.49353
N8	-0.40945	N8	-0.41068	N8	-0.41785	N8	-0.40644	N8	-0.52303
C9	-0.15468	C9	-0.15345	C9	-0.16934	C9	-0.20514	C9	-0.07968
C11	-0.17755	C11	-0.17216	C11	-0.17359	C11	-0.17225	C11	-0.19432
C12	0.562204	C12	0.565002	C12	0.555463	C12	0.550055	C12	0.838474
N15	-0.58223	N15	-0.58693	N15	-0.60092	N15	-0.59857	N15	-0.88234
S16	0.317881	S16	0.325431	S16	0.324292	S16	0.312829	S16	0.386595
O17	-0.44065	O17	-0.43418	O17	-0.42838	O17	-0.42736	O17	-0.5594
C18	0.401804	C18	0.410867	C18	0.331244	C18	0.223132	C18	0.579017
C19	0.120104	C19	0.197289	C19	-0.19692	C19	0.126236	C19	0.041474
C20	0.113592	C20	0.159773	C20	0.165561	C20	0.253123	C20	0.133732
C21	-0.00949	C21	-0.33533	C21	0.004301	C21	-0.03945	C21	0.355276
C23	0.122361	C23	0.08884	C23	0.169288	C23	0.191336	C23	-0.41195
N26	-0.41278	N26	-0.40926	N26	-0.34089	N26	-0.42276	N26	-0.49528
C27	-0.03306	C27	0.167025	Cl27	0.187038	C27	0.022806	Cl27	0.174287

3.3. Molecular electrostatic potential analysis

Molecular electrostatic potential (MEP) is a helpful descriptor used to visualize the electrophilic or nucleophilic reactive sites of molecules [30], and to show the electrostatic potential regions in terms of color grading. In MEP map (**Figs. 2a-e**), different values of the

electrostatic potential are represented by different colors. Potential increases in the order of: red < orange < yellow < green < blue. The positive regions are placed around all hydrogen atoms, which are related to nucleophilic reactivity [30]. The negative regions are located around the oxygen and nitrogen atoms. As we conclude from this our title molecules are ready for both electrophilic and nucleophilic reactions.

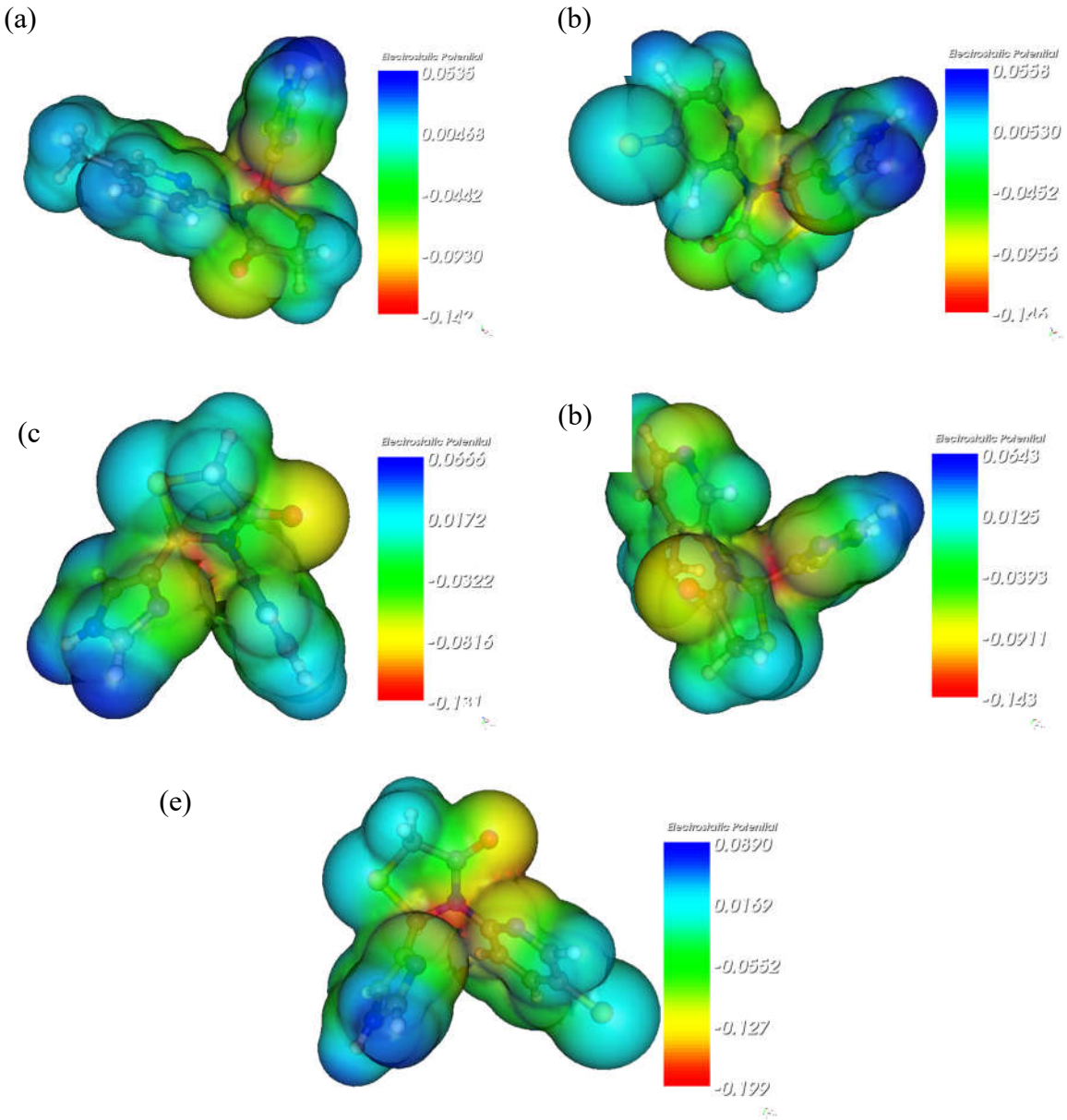

Figs. 2 (a-e) MEP images of compounds **6-10**

3.4. Frontier molecular orbital analysis

On a fundamental level, there are a few different ways to ascertain the excitation energies. The least difficult one includes the difference between the highest occupied molecular orbital (HOMO) and the lowest unoccupied molecular orbital (LUMO) of a organic system, and is a key parameter deciding molecular properties. Both HOMO and LUMO are the fundamental orbital taking part in chemical reaction. The HOMO energy describes the capacity of electron giving, the LUMO portrays the capacity of electron accepting, and the hole among HOMO and LUMO describes the molecular chemical stability [31]. The energy gap between the HOMOs and LUMOs is a basic parameter in deciding molecular electrical transport properties since it is a proportion of electron conductivity [31]. Surfaces for the frontier orbitals were attracted to comprehend the holding plan of present compound. It builds up relationship in different compound and biochemical frameworks [32]. There are parts of uses accessible for the utilization of the HOMO and LUMO energy gap as a quantum chemical descriptor. The HOMO energies, the LUMO energies and the energy gap for the title molecules have been calculated using B3LYP level with 6-31G(d,p) basis set and the results are tabulated in **Table 2**. In the **6-10**, HOMO values are observed in the region -5.90 to -8.86 eV and LUMO values are lie in the region -0.79 to -2.65 eV. As a result, the trend of ΔE gap of inspected compounds becomes **10** > **9**> **6** > **8** > **7**. We can observe from the trend, the introduction of different substituent at pyridine core significantly change the ΔE value.

	HOMO	LUMO
6	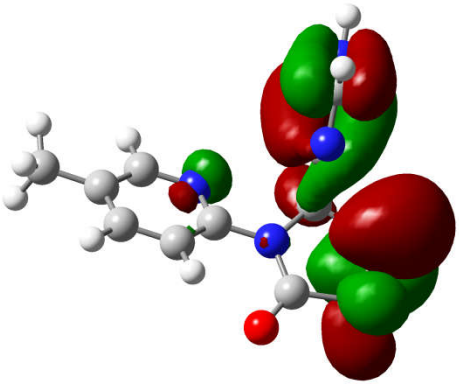	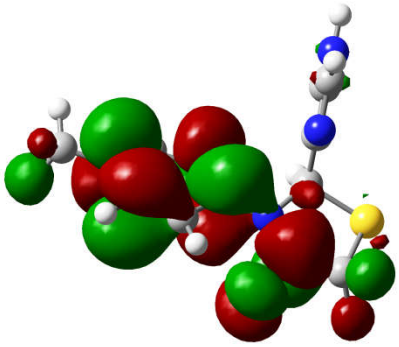
7	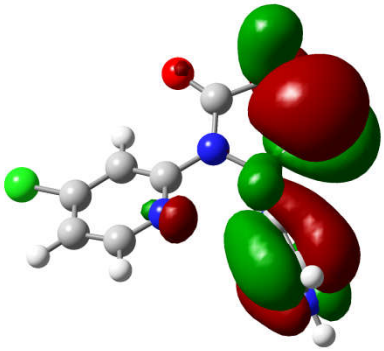	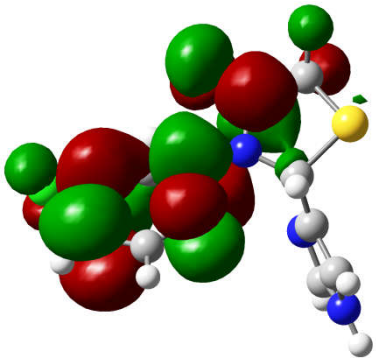
8	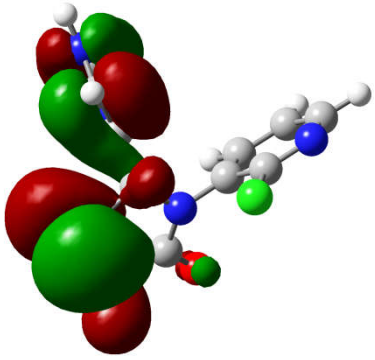	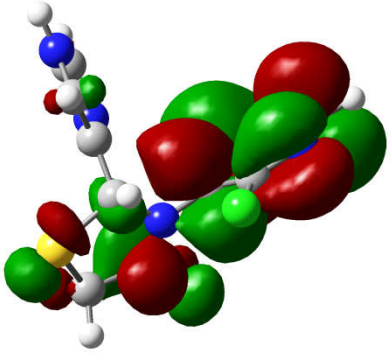

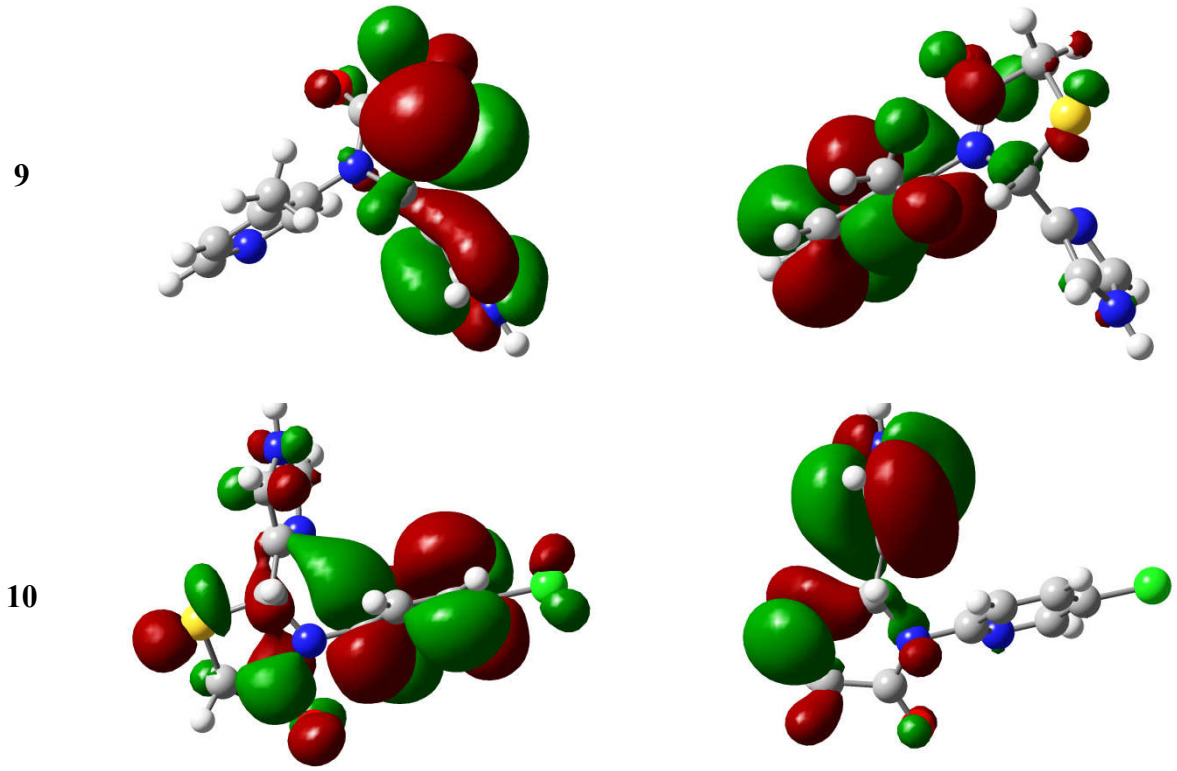

Fig. 3 Molecular orbitals and energies for the HOMO and LUMO in gas phase.

Table 2. Calculated energy values (eV) of **6-10** in gas phase.

DFT-B3LYP/6-31G(d,p)	**6**	**7**	**8**	**9**	**10**
E_{HOMO}	-5.90	-6.06	-6.16	-6.12	-8.86
E_{LUOMO}	-0.79	-1.15	-1.09	-0.80	-2.65
$E_{LUMO-HOMO}$	5.11	4.91	5.08	5.32	6.21
Electronegativity(χ)	-3.35	-3.61	-3.63	-3.46	-5.76
Hardness(η)	2.56	2.46	2.54	2.66	3.11
Electrophilicity index(ψ)	2.19	2.65	2.59	2.25	5.34
Softness(s)	144.83	150.79	145.85	139.22	119.20

As seen from **Fig. 3**, the electron density plots of HOMO electrons are mainly delocalized on the thiazolidine and imidazole rings, while LUMO is spread on pyridine ring in the title compounds. Chemical hardness is related with the stability and reactivity of a chemical

system, it measures the resistance to change in the electron distribution or charge transfer. In this sense, chemical hardness corresponds to the gap between the HOMO and LUMO. The larger the HOMO–LUMO energy gap, the harder, more stable and less reactive the molecule. The higher value of ΔE represents more hardness or less softness of a compound, thus compound **10** referred as hard molecule when compared to **6-9.** Another global reactivity descriptor electrophilicity index describes the electron accepting ability of the systems quite similar to hardness and chemical potential. High values of electrophilicity index increases electron accepting abilities of the molecules. Thus, electron accepting abilities of compounds **6-10** are arranged in following order: **6** > **9** > **7** > **8** > **10**. The softness values follows the **7** > **8** > **6** > **9** > **10**. As seen from the trend compound **7** is the soft molecule.

3.5. Non-linear optical activity

NLO is important property providing key for areas such as telecommunications, signal processing and optical interactions [33,34]. A large variety of NLO switches exhibiting large changes in the first order hyperpolarizability (β), the molecular second-order NLO response. In this context, the design of NLO switches, that is, molecules computed for their first hyperpolarizability by alternate their substitution in phenyl core.

From **Table 3,** the order of dipole moments for **6-10** is **10 > 9 > 8 > 7 > 6**. The dipole moment in a molecule is an important property that is mainly used to study the intermolecular interactions involving the non-bonded type dipole–dipole interactions. Polarizability is proportional with molecular volume. The bigger molecular polarizability means the more interaction with the electric field of light. Thus, molecular electronic charge distributions have been rearranged by interaction with electric field of light. The order of polarizability is **10 > 8 >**

7 > 9 > 6. According to hypolarizability values in table all values of each mentioned molecules are greater than their urea [35] values. Therefore, NLO properties of our compounds are better than urea. Results from NLO Table, The general ranking of NLO properties should be as follows: **10** > **8** > **7** > **9** > **6**. With results in hand, molecule **10** is the best candidate for NLO properties.

Table 3 Non-linear optical properties of **6-10** calculated using B3LYP / 6-31G(d,p) level theory.

NLO behavior	**6**	**7**	**8**	**9**	**10**
Dipole moment (μ) D	5.56	6.10	6.70	7.40	8.25
Polarisability (α) $x10^{-23}$ esu	1.52	1.63	1.66	1.57	1.70
Mean polarisability (Δα) $x10^{-24}$ esu	2.58	2.57	3.24	4.94	1.96
Hyperpolarisability (β_0) $^{x10-30}$ esu	1.25	1.43	1.45	1.41	1.48

4. Conclusion

Overall, operationally simple syntheses were done to give compounds **6-10** in good yield. The optimized structural parameters are analyzed by B3LYP level of theory utilizing 6-31G (d,p) basis set. An examination between the experimental and calculated structure demonstrated a decent correlation. Reactive sites of the title compound were recognized from Mulliken and MEP function analyses. The small ΔE between the HOMO and LUMO of the title compounds inform the happening of ultimate transfer of charge within the molecule. The hyperpolarizability calculation reveals the present material has a reasonably good propensity for nonlinear optical activity. The designed candidates could be utilized for the preparation of NLO crystals which may produce second order harmonic waves.

References

[1] S. Ermer, S.M. Lovejoy, D.S. Leung, H. Warren, Chem. Mater. 9 (1997) 1437.

[2] B.B. Ivanova, M. Spiteller, Cryst. Growth Des. 10 (2010) 2470.

[3] M. Jazbinsek, L. Mutter, P. Gunter, IEEE J. Sel. Top. Quantum Electron. 14 (2008) 1298.

[4] H. Asahi, T. Inabe, Chem. Mater. 6 (1994) 1875.

[5] M.E. Reyes-Melo, J.J. Martinez-Vega, C.A. Guerrero-Salazar, U. Ortiz-Mendez, J. Optoelectr. Adv. Mater. 6 (2004) 1037.

[6] M. V. Diurno, O. Mazzoni, F. Capasso, A. A. Izzo, and A. Bolognese, Farmaco, 52, (1997) 237.

[7] N. Ergenc and G. Capan, Farmaco, 49(1994) 449.

[8] S. Desai, R. Desai, and N. Chandra Desai, "Indian Journal of Ophthalmology, 51(2003) 361.

[9] R. C. Sharma and D. Kumar, Journal of Indian Chemical Society, 77(2000) 492.

[10] E. Piscapo, M. V. Diurno, R. Gagliardi, and O. Mazzoni, Bollettino Della Societa Italiana di Biologia Sperimentale, 65(1989) 853.

[11] H. Ueno, T. Oe, I. Snehiro, and S. Nakamura, "US Patent, 5594116, 1997," Chemical Abstracts, 126 (1977)157507.

[12] T. Previtera, M. G. Vigorita, M. Bisila, F. Orsini, F. Benetolla, and G. Bombieri, European Journal of Medicinal Chemistry, 29(1994) 317.

[13] M. V. Diurno, O. Mazzoni, G. Correale et al., "Farmaco, 54(1999) 579.

[14] M. Y. Ebeid, O. A. Fathallah, M. I. El-Zaher, M. M. Kamel, W. A. Abdon, and M. M. Anwar, "Bulletin of Faculty of Pharmacy, 34(1996) 125.

[15] R. K. Rawal, Y. S. Prabhakar, S. B. Katti, and E. De Clercq, Bioorganic and Medicinal Chemistry, 13(2005) 6771.

[16] R. Ottaná, E. Mazzon, L. Dugo et al., European Journal of Pharmacology, 448(2002) 71.

[17] Ch. Bosshard, K. Sutter, P.H. Pretre, J. Hulliger, M. Florsheimer, P. Kaatz, P. Gunter, Amsterdam, 1995.

[18] H.S. Nalwa, S. Miyata, Nonlinear Optics of Organic Molecules and Polymers, CRC Press, Boca Raton, 1997.

[19] A. Lakhdar Toumi, A. Khelil, K. Tobel, M. Makha, L.A. Hernández, Y. Mouchaal, L. Cattin, M.A. del Valle, F.R. Diaz, J.C. Bernède, Solid-State Electronics 104 (2015) 15.

[20] H Pir Gümüs, Ö Tamer, D Avcı, Y Atalay, E. Tarcan, Braz J Phys,46 (2016) 471.

[21] A. Chouaih, F. Hamzaoui, G. Vergoten, Journal of Molecular Structure 738 (2005) 33.

[22] F. Hamzaoui, A. Zanoun, G. Vergoten, Journal of Molecular Structure 697 (2004) 17.

[23] K. Toubal, N. Boukabcha, Ö. Tamer, N. Benhalima, S. Altürk, D. Avcı, A. Chouaih, Y. Atalay, A. Djafri, F. Hamzaoui, J. Mol. Struct., 1147(2018) 569.

[24] Michal Becka, Maria Vilkova, Michal Soral, Ivan Potocnak, Martin Breza, Tibor Beres, JanImrich, J. Mol. Struct., 1154 (2018) 152.

[25] Salem Yahiaoui, Anna Moliterni, Nicola Corriero, Corrado Cuocci, Khaled Toubal, Abdelkader Chouaih, Ayada Djafri, Fodil Hamzaoui, J. Mol. Struct., 1177 (2018)186.

[26] M. Arockia doss , G. Rajarajan, V. Thanikachalam, S. Selvanayagam, B. Sridhar, J. Mol. Struct., 1128 (2017) 268.

[27] S. Savithiri, M. Arockia doss, G. Rajarajan, V. Thanikachalam, J. Mol. Struct., 1105 (2016) 225.

[28] M.J. Frisch, G.W. Trucks, H.B. Schlegel, G.E. Scuseria, M.A. Robb, J.R. Cheeseman, G. Scalmani, V. Barone, B. Mennucci, G.A. Petersson, H. Nakatsuji, M. Caricato, X. Li, H.P. Hratchian, A.F. Izmaylov, J. Bloino, G. Zheng, J.L. Sonnenberg, M. Hada, M. Ehara, K. Toyota, R. Fukuda, J. Hasegawa, M. Ishida, T. Nakajima, Y.Honda, O. Kitao, H. Nakai, T. Vreven, J.A. Montgomery, Jr., J.E. Peralta, F. Ogliaro, M. Bearpark, J.J. Heyd, E. Brothers, K.N. Kudin, V.N. Staroverov, R. Kobayashi, J. Normand, K. Raghavachari, A. Rendell, J.C. Burant, S.S. Iyengar, J. Tomasi, M. Cossi, N. Rega, J. M. Millam, M. Klene, J.E. Knox, J.B. Cross, V. Bakken, C. Adamo, J. Jaramillo, R. Gomperts, R.E. Stratmann, O. Yazyev, A.J. Austin, R. Cammi, C. Pomelli, J.W. Ochterski, R.L. Martin, K. Morokuma, V.G. Zakrzewski, G.A. Voth, P. Salvador, J.J. Dannenberg, S. Dapprich, A.D. Daniels, O. Farkas, J.B. Foresman, J.V. Ortiz, J. Cioslowski, D.J. Fox, Gaussian 03, Revision C.02, Gaussian Inc., Wallinford, CT, 2004.

[29] M. Arockia doss, S. Savithiri, G. Rajarajan, V. Thanikachalam, C. Anbuselvan, Spectrochim. Acta Part A, 151 (2015) 773.

[30] K. Gokula Krishnan, R. Sivakumar, V. Thanikachalam, H. Saleem, M. Arockia doss, Spectrochim. Acta Part A, 144 (2015) 29.

[31] M. Arockia doss , G. Rajarajan, V. Thanikachalam, S. Selvanayagam, B. Sridhar, J. Mol. Struct., 1158 (2018) 277.

[32] S. Savithiri, M. Arockia doss, G. Rajarajan, V. Thanikachalam, S. Bharanidharan, H. Saleem, Spectrochim. Acta Part A 136 (2015) 782.

[33] M. Arockia doss, S. Savithiri, G. Rajarajan, V. Thanikachalam, H. Saleem, Spectrochim. Acta Part A 148 (2015) 189.

[34] Z.M. Jin, B. Zhao, W. Zhou, Z. Jin, Powder Diffr. J. 12 (1997) 47.